Heimo Huth[1]

Influence of Fastener Flexibility on the Prediction of Load Transfer and Fatigue Life for Multiple-Row Joints

REFERENCE: Huth, H., **"Influence of Fastener Flexibility on the Prediction of Load Transfer and Fatigue Life for Multiple-Row Joints,"** *Fatigue in Mechanically Fastened Composite and Metallic Joints, ASTM STP 927,* John M. Potter, Ed., American Society for Testing and Materials, Philadelphia, 1986, pp. 221–250.

ABSTRACT: An improvement of the accuracy of fatigue life prediction methods used for multiple-row riveted or bolted joints can be expected only if the rivet load distribution is considered during design and fatigue analysis. To calculate the individual load transfer and the bypassing load the fastener flexibility must be taken into account. Semiempirical formulas for the calculation of fastener flexibility existing in the literature turn out to be not exact or at least not applicable for a wider range of joint geometries. This unsatisfactory situation was the reason for performing an extensive experimental investigation during which fastener flexibilities for a wide range of joints of practical interest were determined.

The effects of primary joint parameters, such as the plate material, clamping length, and diameter and material of the fastener, as well as the effects of secondary parameters, such as the clamping force, condition of the faying surfaces, and fit and type of head of the fastener, were investigated through specific variations. For this purpose load-deformation measurements under quasi-static and flight-by-flight loading conditions were performed using single- and double-shear specimens with known load transfer.

A formula for fastener flexibility, valid for riveted and bolted metallic and graphite/epoxy joints, was derived from the test results and proved to be significantly superior to those found in the literature. This formula for load transfer calculations of multiple-row fatigue loaded joints was used to predict accurately the measured values of load transfer. This improvement also leads to a better fatigue life prediction. The load transfer measurements showed a quasi-linear relationship between the applied load and the total load transfer which was little affected by fatigue loading, although the load transferred by bearing was not constant. By measuring bearing loads and local strains close to fastener holes in a multiple-row joint the author shows that with increasing friction the bearing stress and the local strains decreased. The redistribution of loads or the changes in the mechanisms of load transfer result in a relief of the fatigue critical location. Since these changes of the local stress situation cannot be predicted, the application of fatigue life prediction methods on the basis of local strains must lead to inaccurate results.

[1] Research engineer, Fraunhofer-Institute fuer Betriebsfestigkeit (LBF), Darmstadt, West Germany.

KEY WORDS: fastener flexibility, load transfer, riveted joint, bolted joint, single-shear joint, double-shear joint, fatigue life estimation, Falstaff sequence, graphite/epoxy, aluminum alloy, deformation measurements

By far, most of the fatigue cracks occurring in aircraft structures originate at holes of shear loaded fasteners. This is due mainly to the inaccuracy of fatigue life prediction methods used for multiple-row riveted or bolted joints. The three main causes for this inaccuracy are the following:

1. The damage accumulation hypothesis itself is inaccurate.
2. The design data are not appropriate.
3. Mistakes are made during stress analysis.

The aim of this investigation was to show how the last two problems can be alleviated. For this purpose it is essential to determine and correctly consider the forces/stresses acting in a joint. As shown in Fig. 1 for the last fastener of a single-shear joint, the stresses result from these forces:

(*a*) the bypassing force, F_{BP},
(*b*) the bearing force, F_{BR}, and
(*c*) the forces transferred by friction, F_{FR}.

The last two forces sum up the total load transferred at that fastener location, F_{LT}. If this force, often also referred to as rivet force, is related to the applied external force, F_0, one talks of the "load transfer." Although it is well known that the amount of load transfer has a superior influence on

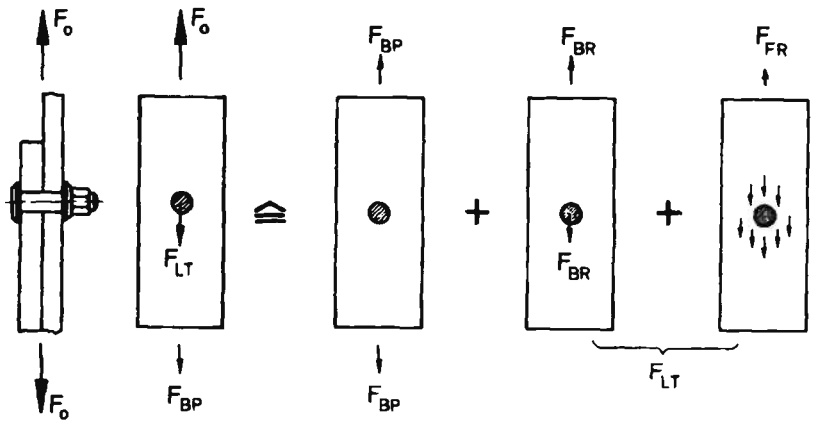

FIG. 1—*Definition of forces acting in a joint.*

the fatigue life of a multiple-row joint, surprisingly few results of investigations can be found in the literature [*1–3*]. For example, the *S-N* curves for single-shear riveted joints derived from test results reported in Ref *1* are shown in Fig. 2. The amount of load transfer was varied from 22 to 100% by changing the number of rivets from 10 to 1. It can be seen that in the region of practical interest ($0.2 < LT < 0.5$) there is a factor of 10 on the fatigue life.

Load transfer or the distribution of rivet loads in a multiple-row joint depends not only on the number of rivets used but even more on the fastener flexibility. If the rivet loads are to be calculated, using, for example, a mathematical model developed in Refs *4* and *5* and extended in Ref *6*, the stiffness of flexibility of the rivets has to be considered. As shown schematically in Fig. 3, the fastener flexibility has a more or less pronounced influence, depending on the type of joint in question.

In the aircraft industry a number of semi-empirical formulas for the calculation of fastener shear flexibility have been developed [*7–10*]. In most cases they were derived from a rather limited number of static tests. A comparison of the different formulas has been presented in Refs *11* and *12*. The results were disappointing since the scatter was rather large and, furthermore, a comparison of test results of flight-by-flight loaded specimens showed large differences in fastener flexibilities.

This unsatisfactory situation was the reason for performing an extensive experimental investigation during which fastener flexibilities for a wide range of joints of practical interest were to be determined.

Experimental Determination of Fastener Flexibilities

The following parameters were expected to affect the deformation behavior and thus also the fastener flexibility. The primary parameters (dealing with geometry and materials) are the following:

(*a*) Young's modulus of the plate materials,
(*b*) clamping length,
(*c*) fastener diameter,
(*d*) fastener material, and
(*e*) single- or double-shear configuration.

The secondary parameters (dealing with installation) are these:

(*a*) clamping force,
(*b*) fit of the fastener,
(*c*) type of fastener head, and
(*d*) condition of the faying surfaces.

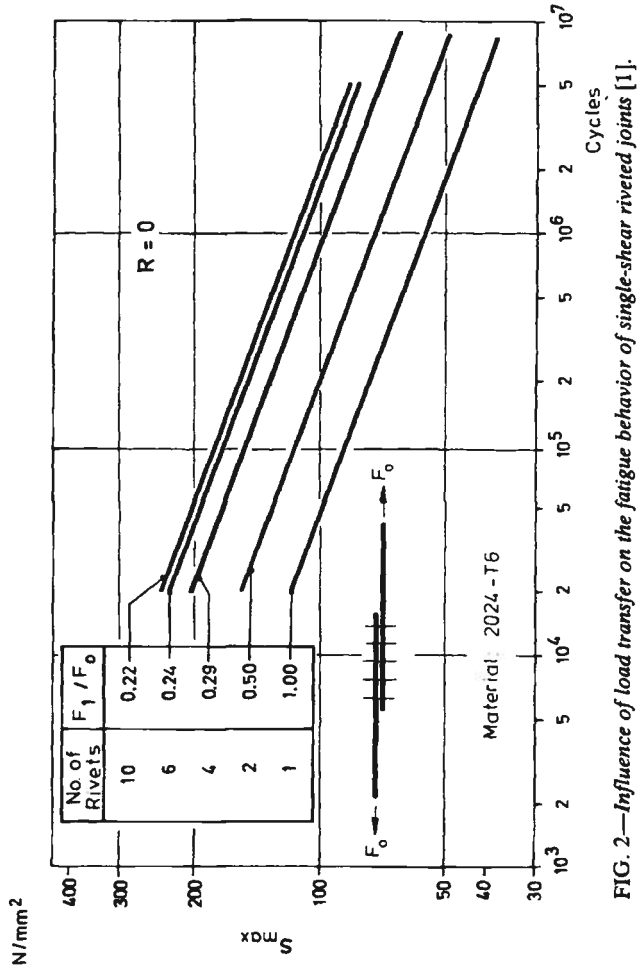

FIG. 2—*Influence of load transfer on the fatigue behavior of single-shear riveted joints* [1].

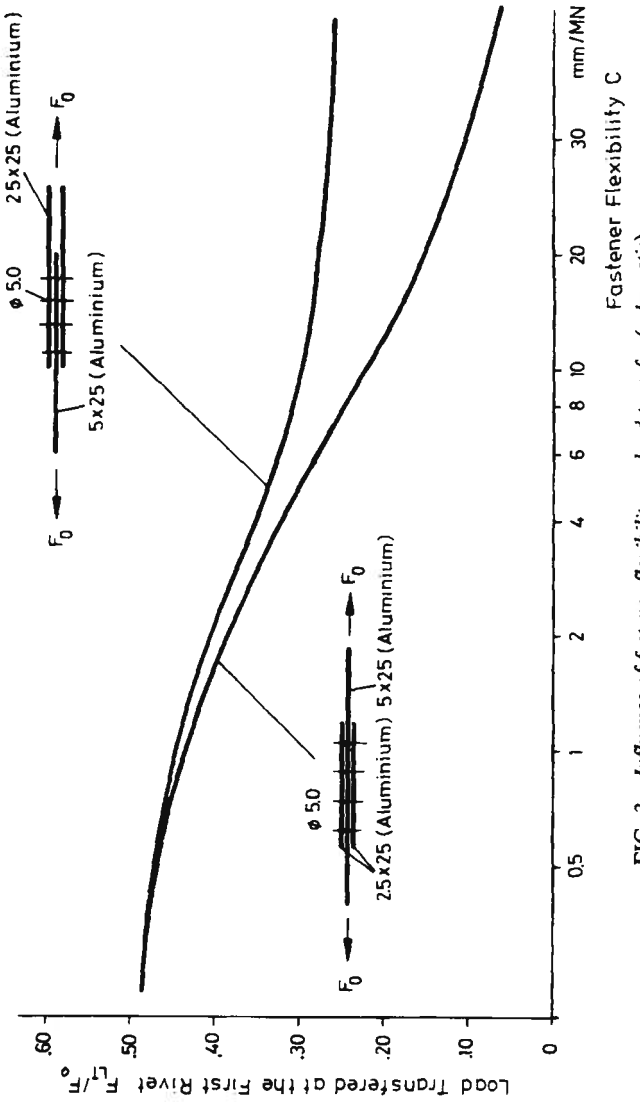

FIG. 3—*Influence of fastener flexibility on load transfer (schematic).*

TABLE 1*a*—*Investigation of Specimens ISS01 and IDS01 of Group I (bolted metallic joints).*

Parameters	Single Shear ISS01	Double Shear IDS01
Primary		
plate materials	2024 T3	2024 T3
fastener material	Ti-6Al-4V	Ti-6Al-4V
clamping length	10 mm	10 mm
bolt diameter	5.0 mm	5.0 mm
Secondary		
type of head	flush head	protruding head
faying surfaces	PRC[a]	PRC[a]
fastener fit	interference fit	interference fit
clamping force	normal (high)	normal (high)

[a] PRC stands for antifretting compound.

In addition, the following three groups of joints of practical interest were defined:

Group I—bolted metallic joints.
Group II—riveted thin-sheet metallic joints.
Group III—bolted graphite/epoxy joints.

Specimens

For each group, two types of basic specimens, single-shear (SS) with 100% and double-shear (DS) with 50% load transfer, were defined using the most common combination of parameters. All other specimens differed by variation of only one primary or secondary joint parameter in the range of practical interest. This is shown in Tables 1*a* and 1*b* for the bolted metallic joints. In all, 45 different specimens were manufactured and tested.

TABLE 1*b*—*Investigation of further specimens of Group I (bolted metallic joints).*[a]

	Single Shear Specimens		Double Shear Specimens	
Parameter V	Results	Specimen No.	Results	Specimen No.
Plate materials	7075 T73	ISS02		
	Ti-6Al-4V	ISS03	Ti-6Al-4V	IDS03
Fastener material	steel	ISS12	steel	IDS10
Clamping length, mm	5.0	ISS05	4.5	IDS05
	20.0	ISS06	15.0	IDS06
			20.0	IDS07
Bolt diameter, mm	6.35	ISS10	6.35	IDS09
	8.0	ISS09	8.0	IDS08
Type of head	protruding head	ISS11	. . .	. . .
Faying surfaces	without PRC	ISS04	without PRC	IDS04
Fastener fit	clearance fit	ISS13	clearance fit	IDS11
Clamping force	low	ISS14	low	IDS12

[a] Additional specimens with blind bolts (ISS15 and IDS13) were tested.

The manufacturing details for Group I include the following: Three different plate materials (2024 T3, 7075 T73, and Ti-6Al-4V alloys) were used; the plate thickness varied between 1.0 and 10.0 mm. For most specimens the sealing compound PR 1436 was applied to the faying surfaces. The fasteners (NAS and Hi-Lok bolts) were installed with interference fit (25 to 30 μm) using normal clamping forces.

The specimens of Group II were made of 2024 T3 clad material using solid rivets and PR 1436.

For the graphite/epoxy specimens of Group III the material T 300/C 914 was used in two lay-ups—Laminate II $(O_2/\pm 45/O_2/\pm 45/\overline{90})_s$ and isotropic $(0/\pm 45/90/0/\pm 45/90)_s$—with nominal thicknesses of 2.1, 4.2, and 6.3 mm. Here the NAS bolts were installed with clearance fit, and a shim of 0.2 mm thickness (Hysol EA 934 ± 50% aluminum powder) was applied to the faying surfaces.

The actual dimensions for those specimens used to investigate the influences of the primary joint parameters, and further details, are listed in Tables 2 and 3.

Test Procedure

Since an experimental determination of the individual deformations due to shear, bending, and bearing loads is not possible, an integral value of the total deformation was measured using a strain-gage-equipped extensometer, as shown in Fig. 4. The elastic deformations of the specimen segments within the gage length, t_0 (Δt_1 and Δt_2), were eliminated by electric compensation, thus the load-δ-curves could be recorded directly.

One specimen of each type was used for quasi-static measurements, being cyclically loaded at $R = 0$ with a stepwise increasing upper load until fracture; thus the elastic-plastic load-deformation curves were obtained.

A second specimen was used to measure the deformations and changes of the deformation behavior under Falstaff loading [*13*]. For these measurements a relatively short artificial flight (11 cycles) was deduced from the Falstaff sequence (see Fig. 5), comprised of load levels 3 to 29 ($\overline{R} = -0.24$). This extra measuring flight was applied as Flights 1 and 2 prior to the Falstaff sequence. After 600 and 6000 flights, the measurements were repeated. Test stress levels were chosen so that a fatigue life of about 12 000 flights could be reached. In some cases, fatigue cracks developed in the single-shear specimens before reaching 6000 flights. For the double-shear specimens, this stress level of $\overline{\sigma}_0 = 172.5\ \mathrm{N/mm^2}$ resulted in somewhat unrealistic high bearing stresses. Thus several tests were repeated using two thirds of this value.

Test Results

From the test results, that is, the recorded load-deformation curves (see the example in Fig. 6), some general phenomena can be derived. The load-

TABLE 2—*Details for the double-shear specimens (variation of primary joint parameters).*

Specimen No.	Materials		Dimensions, mm			Fasteners		Results of the quasi-stat. tests		Fastener Flexibilities, mm/MN		
	1	2	t_1	t_2	w	d	Type	FM	F_{ult}, N	$C_{2/3}$	Falstaff-tests C_F	$\overline{C_F}$
IDS01	2024 T3	2024 T3	5.1	2.5	25	5.0	A 1	X/Y2	22,400	9.6	9.0	5.2
IDS03	Ti 6Al 4V	Ti 6Al 4V	5.4	2.5	25	5.0	A 1	Z	29,800	7.0	6.6	4.6
IDS05	2024 T3	2024 T3	2.5	1.0	25	5.0	A 1	X/Y2	9,800	13.2	12.0	5.0
IDS06	2024 T3	2024 T3	5.1	5.1	25	5.0	A 1	X/Y1	24,500	8.6	8.2	5.4
IDS07	2024 T3	2024 T3	10.1	5.1	25	5.0	A 2	Z	31,120	8.3	7.1	3.6
IDS08	2024 T3	2024 T3	5.1	2.5	40	8.0	A 1	X2	36,980	6.9	6.4	3.8
IDS09	2024 T3	2024 T3	5.1	2.5	32	6.35	A 1	X2	29,250	8.6	8.1	7.7
IDS10	2024 T3	2024 T3	5.1	2.5	25	5.0	B 1	XY/2	23,175	8.6	7.9	6.0
IDS13	2024 T3	2024 T3	5.1	2.5	25	4.8	B 3	X2	22,075	-	8.3	11.2
IIDS01	2024 T3	2024 T3	2.0	1.0	24	4.8	C 1	X2	8,100	17.8	14.2	12.6
IIDS02	2024 T3	2024 T3	4.0	2.0	24	4.8	C 1	Z	10,400	10.4	8.2	5.0
IIDS03	2024 T3	2024 T3	2.0	2.0	24	4.8	C 1	X/Y1	8,750	13.4	-	-
IIDS04	2024 T3	2024 T3	2.0	1.0	16	3.2	C 1	Z	4,130	18.8	17.2	12.0
IIIDS01	CFRP (lam II)	CFRP (lam II)	4.5	2.1	25	5.0	A 1	X2	17,970	15.7	14.8	5.4
IIIDS02	CFRP isotropic	CFRP isotropic	3.8	1.95	25	5.0	A 1	X2	18,940	17.5	15.8	7.4
IIIDS03	CFRP (lam II)	2024 T3	4.4	2.5	25	5.0	A 1	X/Y1	17,080	13.8	11.4	3.4
IIIDS10	CFRP (lam II)	CFRP (lam II)	6.4	4.4	25	5.0	A 1	XY1	28,160	11.1	12.0	3.6

Types of Fasteners:
A = Titanium Bolt
B = Steel Bolt
C = Aluminum Rivet

1 = Protruding Head
2 = Flush Head
3 = Blind Bolt with Prot. Head
4 = Blind Bolt with Flush Head

Failure Modes (FM):

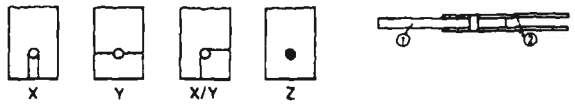

TABLE 3—*Details for the single-shear specimens (variation of primary joint parameters).*

Specimen No.	Materials		Dimensions, mm			Fasteners		Results of the quasi-stat. tests		Fastener Flexibilities, mm/MN		
	1	2	t_1	t_2	w	d	Type	FM	F_{ult}, N	$C_{2/3}$	Falstaff-tests C_F	Falstaff-tests $\overline{C_F}$
ISS01	2024 T3	2024 T3	5.1	5.1	25	5.0	A 2	Z	28,655	24.1	22.0	10.1
ISS02	7075 T3	7075 T3	4.9	4.8	25	5.0	A 2	Z	27,970	25.2	22.4	11.6
ISS03	Ti 6Al 4V	Ti 6Al 4V	5.3	5.3	25	5.0	A 2	Z	29,800	15.2	19.4	10.8
ISS05	2024 T3	2024 T3	2.5	2.5	25	5.0	A 2	Z	15,060	36.0	26.0	11.6
ISS06	2024 T3	2024 T3	10.1	10.1	25	5.0	A 2	Z	32,380	20.6	19.0	13.4
ISS09	2024 T3	2024 T3	5.1	5.1	40	8.0	A 2	Z	>47,800	15.8	13.1	6.3
ISS10	2024 T3	2024 T3	5.1	5.1	32	6.35	A 2	Z	43,155	20.6	20.6	20.2
ISS12	2024 T3	2024 T3	5.1	5.1	32	6.35	B 2	Z	50,210	18.0	15.8	10.9
ISS15	2024 T3	2024 T3	5.1	5.1	25	4.8	B 4	Z	31,815	22.8	24.0	37.0
IISS01	2024 T3	2024 T3	2.0	2.0	24	4.8	C 2	Z	7,700	32.0	28.5	12.4
IISS02	2024 T3	2024 T3	4.0	4.0	24	4.8	C 2	Z	10,600	20.8	19.0	11.8
IISS04	2024 T3	2024 T3	2.0	2.0	16	3.2	C 2	Z	4,080	56.0	55.2	57.6
IISS09	2024 T3	2024 T3	2.0	2.0	24	4.0	C 2	Z	8,250	40.2	36.5	33.6
IIISS01	CFRP (lam II)	CFRP (lam II)	4.5	4.5	25	5.0	A 2	X1	22,020	33.2	30.5	8.0
IIISS02	CFRP isotropic	CFRP isotropic	3.8	3.8	25	5.0	A 2	Y1	19,210	38.6	33.2	8.8
IIISS07	CFRP (lam II)	CFRP (lam II)	4.4	4.4	40	8.0	A 2	Z*	41,740	23.7	21.2	6.8
IIISS08	CFRP (lam II)	CFRP (lam II)	2.2	2.1	25	5.0	A 2	X1/Z	13,104	42.5	52.5	19.8
IIISS09	CFRP (lam II)	CFRP (lam II)	6.4	6.4	25	5.0	A 2	X1	27,030	21.0	28.8	7.6

Types of Fasteners:
A = Titanium Bolt
B = Steel Bolt
C = Aluminum Rivet

1 = Protruding Head
2 = Flush Head
3 = Blind Bolt with Prot. Head
4 = Blind Bolt with Flush Head

Failure Modes (FM):

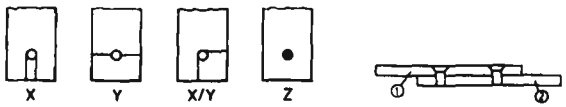

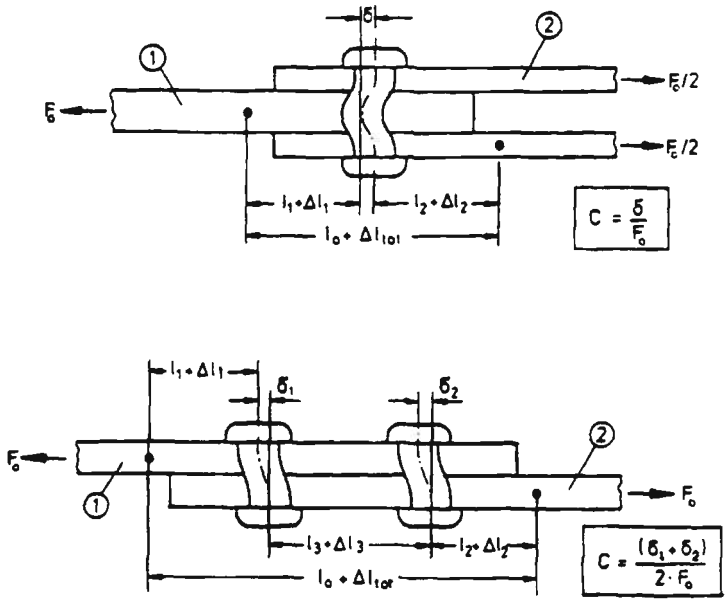

FIG. 4—*Deformations in single- and double-shear specimens.*

deformation curves under static loading (enveloping curve) show a somewhat unexpected behavior since no linear relationship, even in the region of elastic deformations, was recorded. The exceptions are some of the curves recorded with riveted specimens (Group II), probably because of their lower clamping forces. The unloading and reloading curves, however, show a linear behavior with nearly unchanging slope. Having been loaded to a certain amount of permanent deformation, the slope changes only insignificantly until final fracture.

The typical appearance of hysteresis curves recorded during flight-by-flight loading is the following: Due to the rather high but nevertheless realistic stress level, pronounced plastification effects occur during the first flight. The hysteresis loops of the second flight are already much more narrow: with an increasing number of flights their areas increase, while the deformation amplitude gets smaller. The sometimes drastic changes of shape and area are caused by the changing conditions of friction and plastic deformations of the fastener holes. It can be observed, however, that the slope of the linear part of the hysteresis does not change very much. As shown in Fig. 7, the slope of the connecting line between the maximum and minimum of the 0 to 5 *g* loop, $\overline{C}_F$, is strongly influenced by fatigue loading, whereas the slope of the linear part, C_F, is not. A complete presentation of the test results is given in Ref *14*.

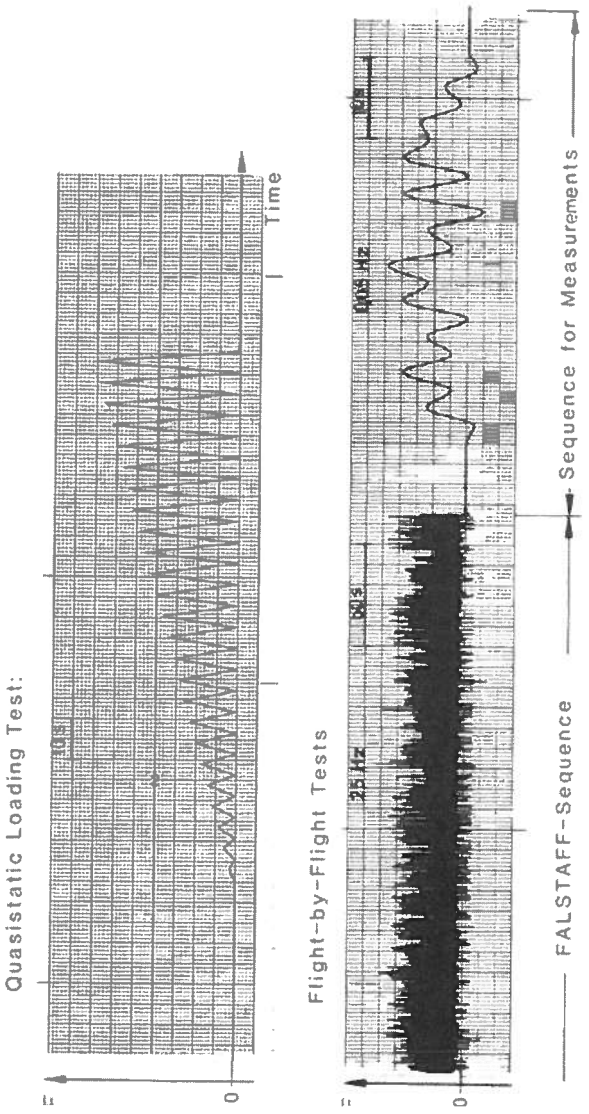

FIG. 5—*Loading sequences used during displacement measurements.*

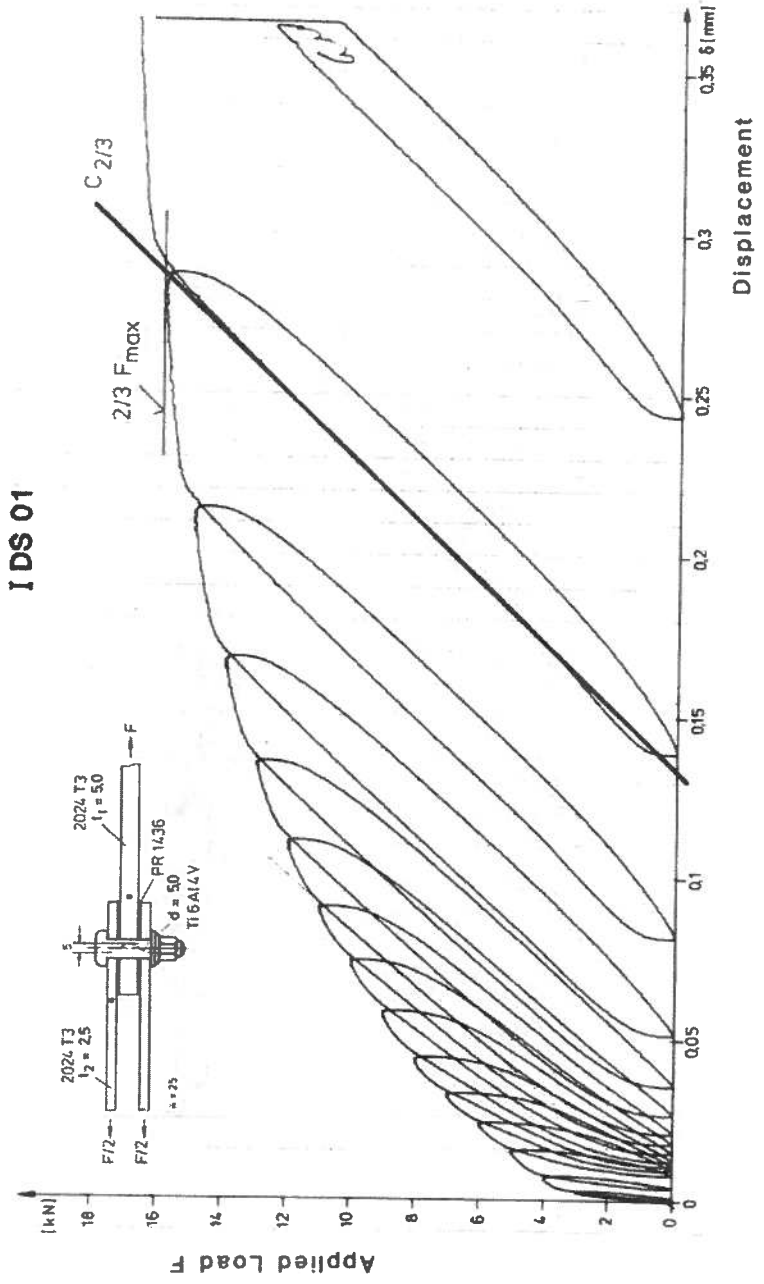

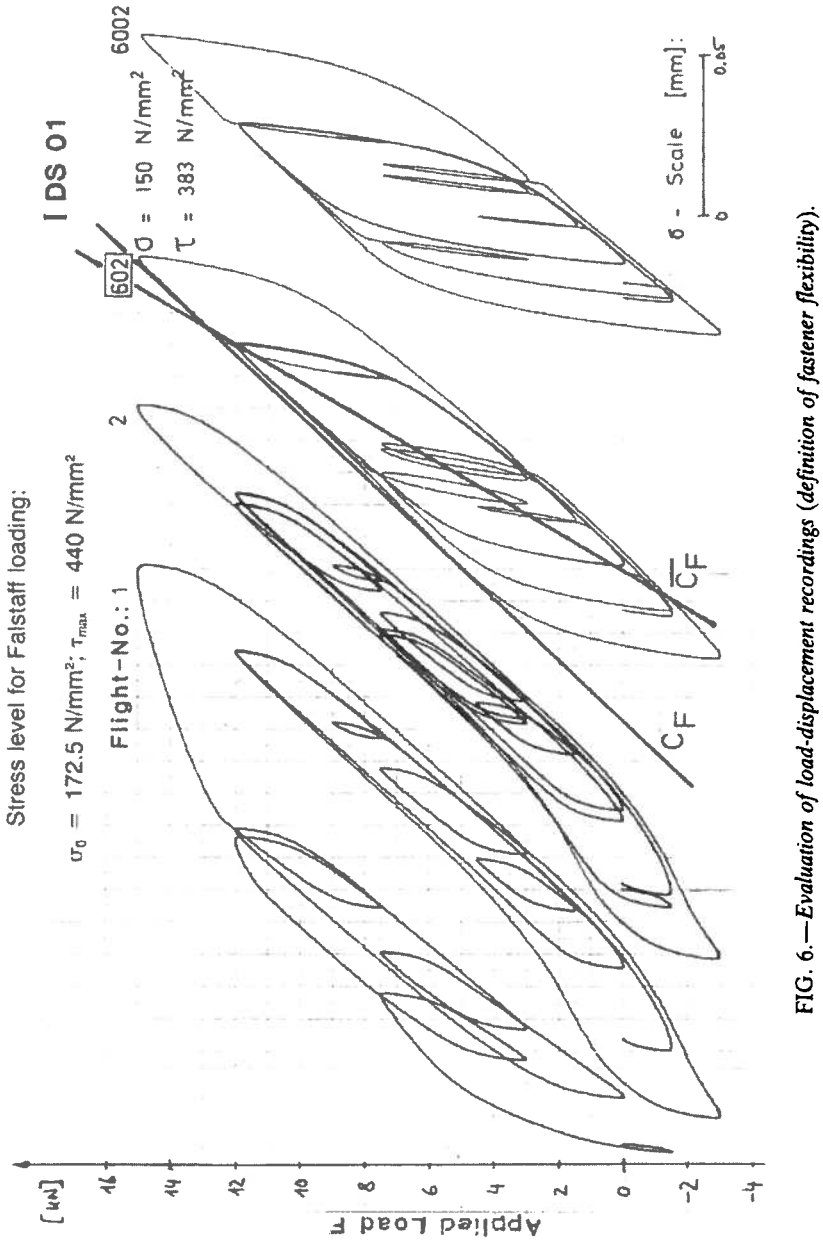

FIG. 6.—*Evaluation of load-displacement recordings (definition of fastener flexibility).*

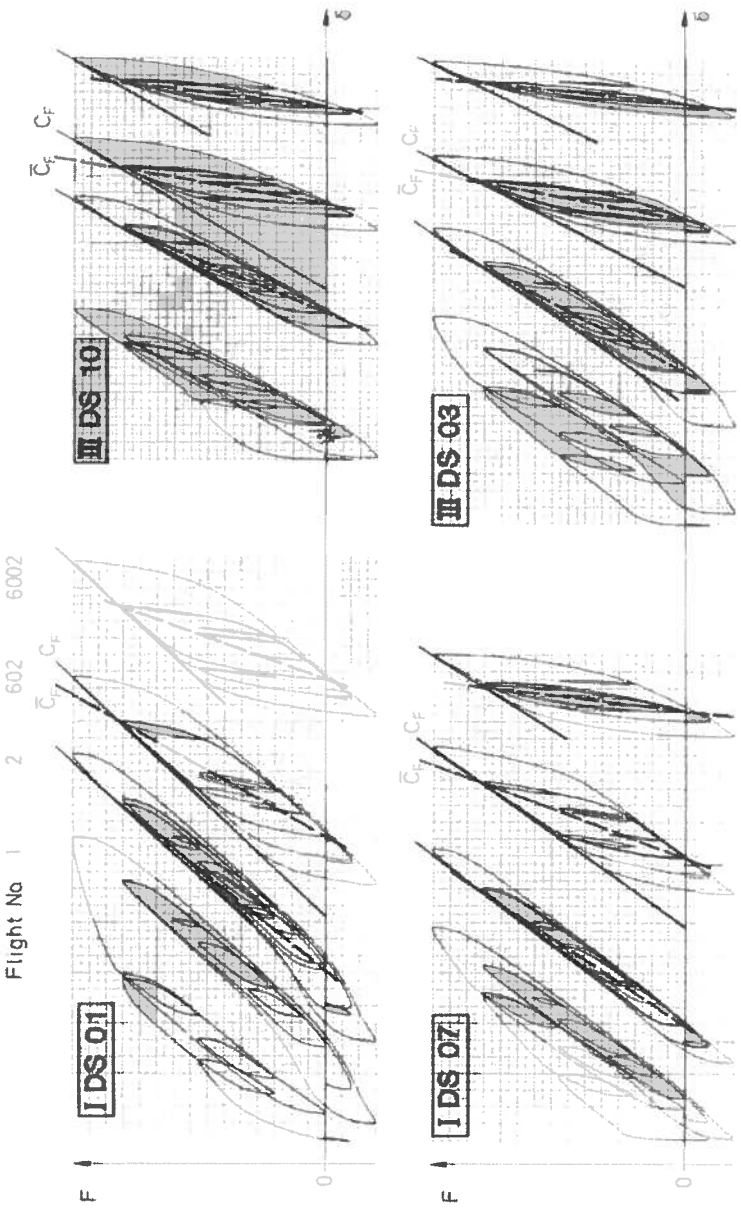

FIG. 7.—*Influence of flight-by-flight loading on fastener flexibility C_f and $\bar{C}_f$ (double-shear specimens).*

Since these C_F values are in most cases identical with the $C_{2/3}$ values of the quasi-static tests (see Fig. 6), the author concludes that these values represent characteristic quantities related to the fastener flexibility of the individual joints.

An equation containing all primary parameters was set up and fitted to the above-mentioned test results, producing a new formula for fastener flexibility:

$$C = \left(\frac{t_1 + t_2}{2d}\right)^a \frac{b}{n}\left(\frac{1}{t_1E_1} + \frac{1}{nt_2E_2} + \frac{1}{nt_1E_3} + \frac{1}{2nt_2E_3}\right) \tag{1}$$

The bracket on the right side comprises the flexibility resulting from bearing loads, while the left part contains portions due to fastener bending and shear. It was necessary to use different Constants a and b for the three groups of joints under consideration:

Group I—bolted metallic joints	$a = 2/3$; $b = 3.0$
Group II—riveted metallic joints	$a = 2/5$; $b = 2.2$
Group III—bolted graphite/epoxy joints	$a = 2/3$; $b = 4.2$

Equation 1 is valid for single-shear ($n = 1$) and double-shear ($n = 2$) joints.

In order to compare the accuracy in predicting fastener flexibilities, the following three equations (for single shear) were chosen from the literature:

Tate and Rosenfeld [*4*]:

$$C = \frac{1}{t_1E_1} + \frac{1}{t_2E_2} + \frac{1}{t_1E_3} + \frac{1}{t_2E_3} + \frac{32(t_1 + t_2)(1 + \nu)}{9E_3\pi d^2} + \frac{8(t_2^3 + 5t_2^2t_1 + 5t_2t_1^2 + t_1^3)}{5E_3\pi d^4} \tag{2}$$

Boeing [*7*]:

$$C = \frac{2^{(t_2/d)^{0.85}}}{t_1}\left(\frac{1}{E_1} + \frac{3}{8E_3}\right) + \frac{2^{(t_2/d)^{0.85}}}{t_2}\left(\frac{1}{E_2} + \frac{3}{8E_3}\right) \tag{3}$$

Douglas [*10*]:

$$C = \frac{5}{d \cdot E_3} + 0.8\left(\frac{1}{t_1E_1} + \frac{1}{t_2E_2}\right) \tag{4}$$

The results of comparative calculations and their comparison with the presented test results are shown in Figs. 8 through 11. For the double-shear case, equations from the literature predict values that are too high, which would lead to an overestimation of fatigue life. For single-shear specimens, the opposite tendency can be noticed.

Load Transfer Measurements and Calculations

In order to test the applicability of the derived Eq 1 for fastener flexibility, load transfer measurements with several different multiple-row joints were performed. Thus, the possible improvements in load transfer calculation were to be demonstrated. Thirteen different types of strain-gage specimens—four examples are shown in Fig. 12—were used for load transfer measurements. The load transfer at the first fastener ranged between 15% and 45%. Special attention was paid to a correct positioning of the strain gages, since strain distributions across the width of the specimen, as shown on Fig. 13, were expected and had to be taken into account.

For some specimens, the measurements were repeated after the application of some 600 flights of the Falstaff loading sequence. For lap joints, the fatigue loading does not result in changes of load transfer and fastener load distribution, as shown on Fig. 14. Moderate changes are recorded for reinforcement specimens (Types II.1 and II.2), but in general a quasi-linear relationship between the transferred load and the applied load is obtained.

Comparisons between the calculated and measured load transfer values resulted in good agreement (Fig. 15). The application of the so-called Boeing and Douglas formulas (Eqs 3 and 4) during load transfer calculations for the specimens investigated led in some cases to errors of 40%, as shown on Fig. 16. From available fatigue test results it can be concluded that such errors in load-transfer predictions would result in a 400% error for the predicted fatigue life.

Mechanisms of Load Transfer

In order to clarify the discrepancies between the results of the deformation measurements that show a distinct influence of fatigue loading on the deformation behavior and the results of the load-transfer measurements where this influence does not appear, some additional tests were performed. A double-shear specimen with three fasteners (Fig. 17) was prepared to measure load transfer, the local strain at a fastener hole, the bearing load, and the displacement (that is, fastener flexibility) simultaneously. The total load transfer was measured using three strain gages positioned between two fasteners, and the load transferred by bearing was measured using an instrumented steel bolt. The results obtained are shown on Fig. 18. It can be seen that all curves except that of the total load transfer show a clear

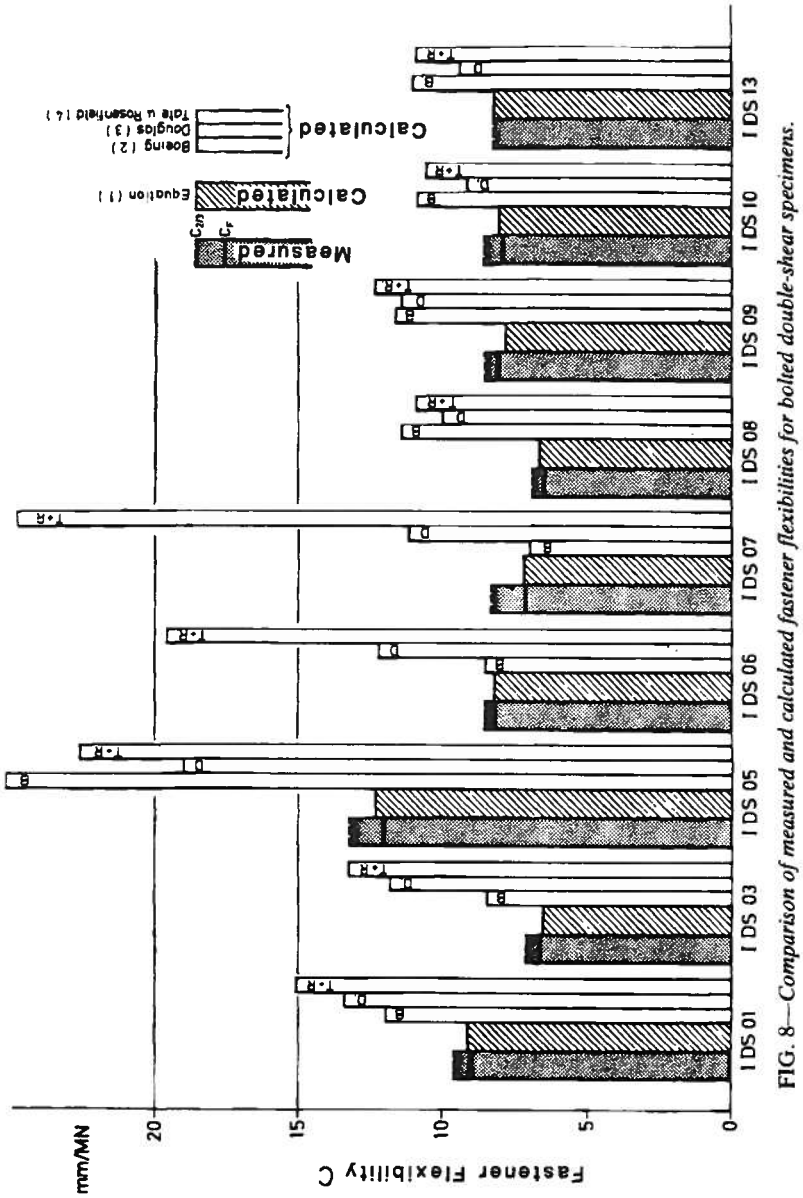

FIG. 8—*Comparison of measured and calculated fastener flexibilities for bolted double-shear specimens.*

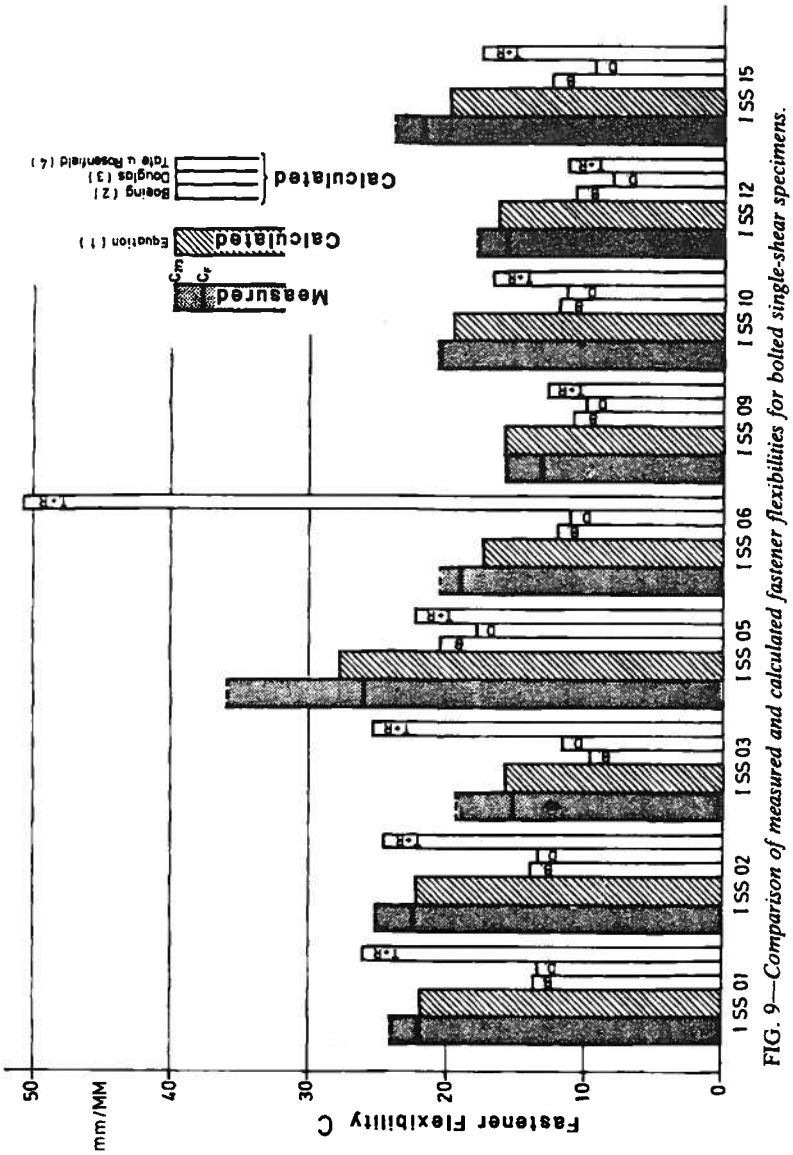

FIG. 9—Comparison of measured and calculated fastener flexibilities for bolted single-shear specimens.

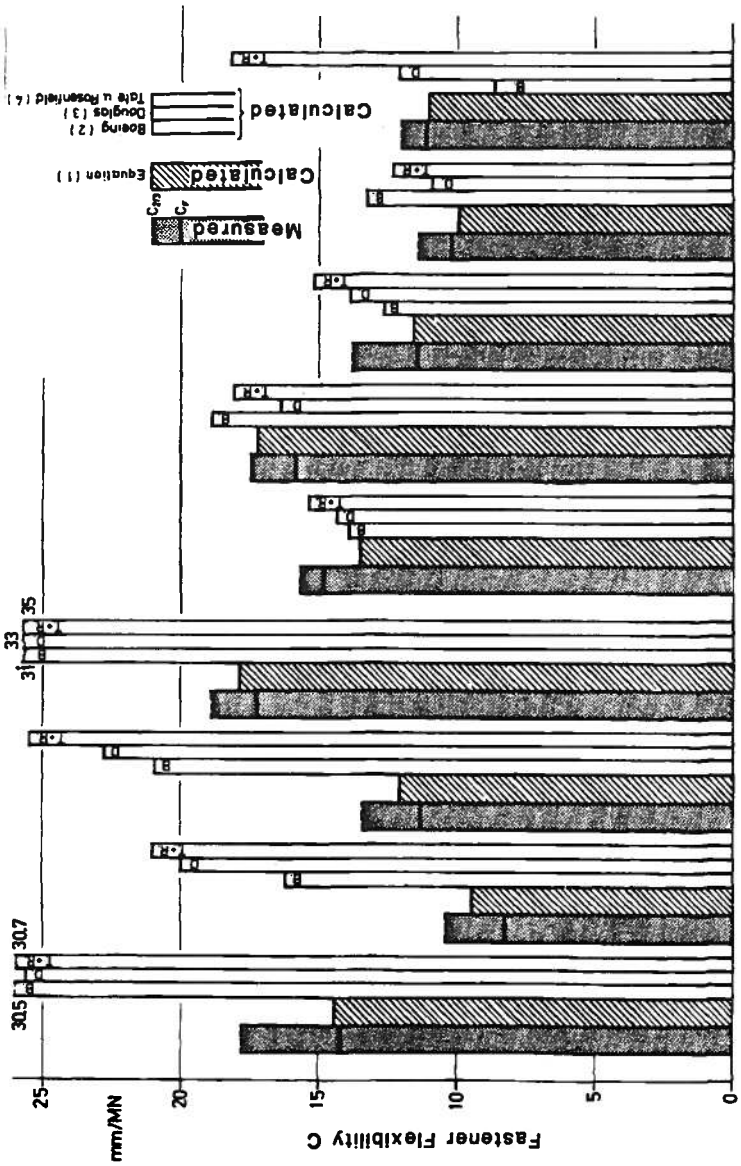

FIG. 10—*Comparison of measured and calculated fastener flexibilities for riveted metallic and bolted graphite/epoxy double-shear specimens.*

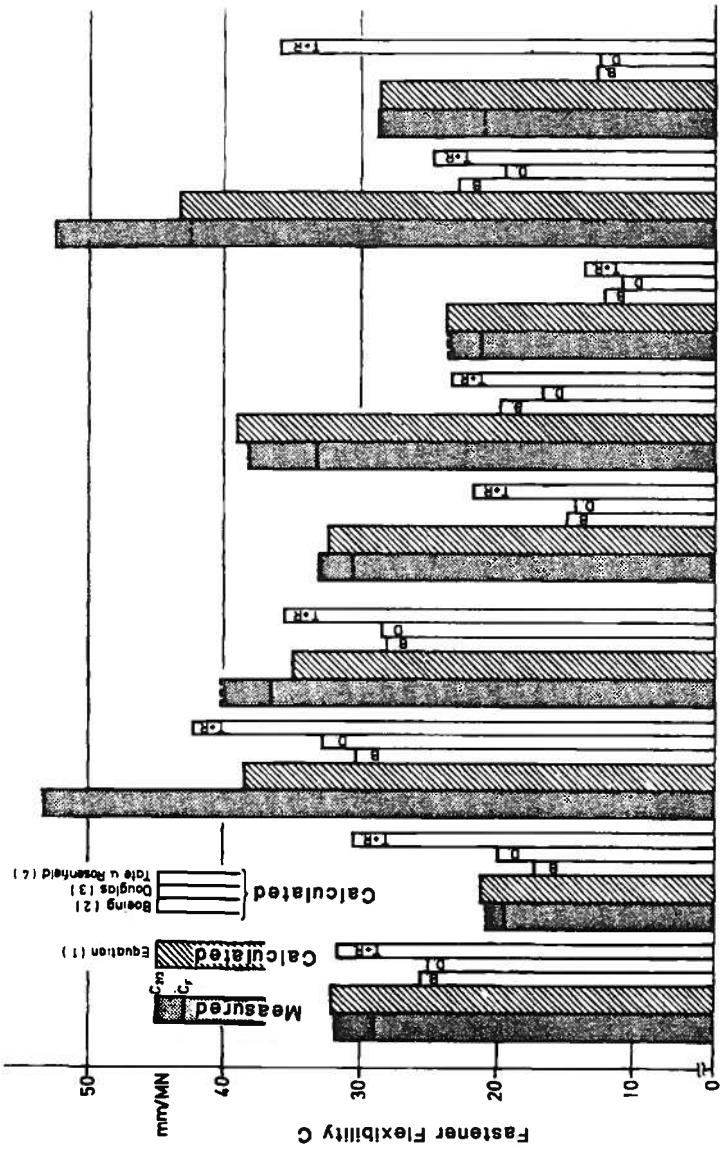

FIG. 11—*Comparison of measured and calculated fastener flexibilities for riveted metallic and bolted graphite/epoxy single-shear specimens.*

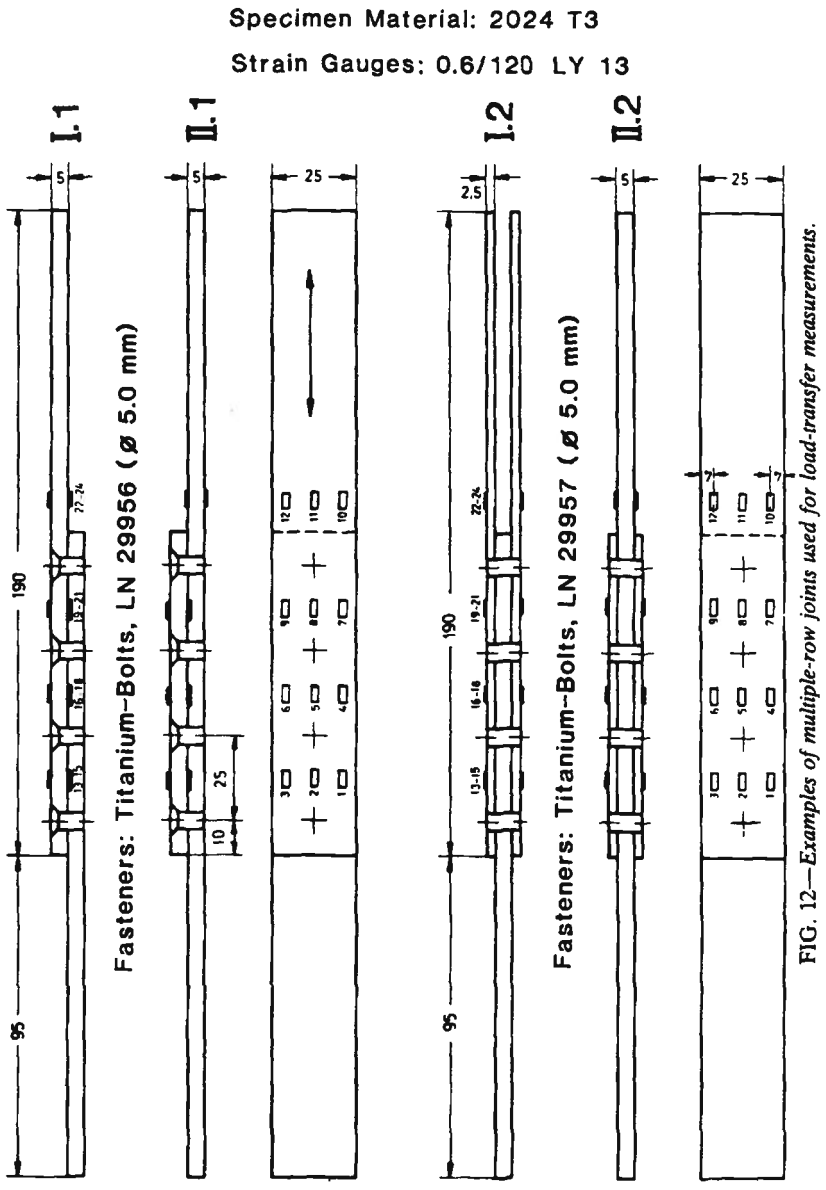

FIG. 12—*Examples of multiple-row joints used for load-transfer measurements.*

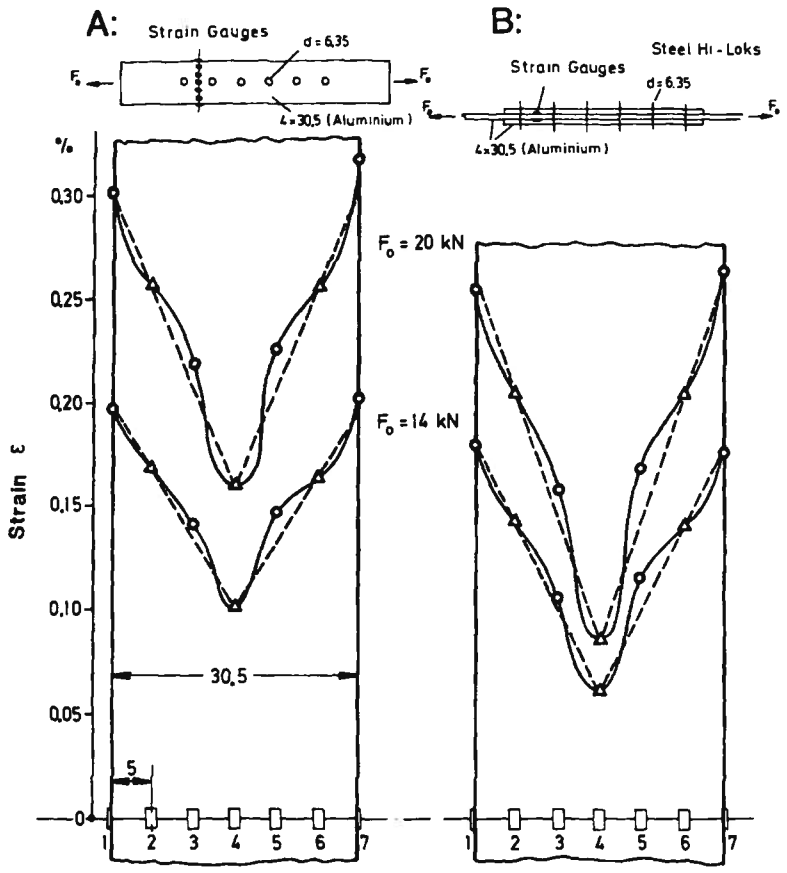

		$\bar{\varepsilon}$ [%]	S [N/mm²]	F_0 [N]
A	—— 12 Str. Gauges	0.231	161.5	19,702
	– – – 3 Str. Gauges	0.230	161.0	19,642
	from F_0/A_{Gross}	–	163.9	20,000
B	—— 12 Str. Gauges	0.1732	121.2	14,791
	– – – 3 Str. Gauges	0.1730	121.1	14,770

Δ: Recommended Strain Gauges Positions

FIG. 13—*Experimental determination of load transfer from measured strain distributions.*

nonlinear behavior. The recorded changes of slope occur at about the same level of applied load.

Taking into account the results of the fastener flexibility measurements—in particular, the changes of the hysteresis loops with increasing number of flights—the following statements about the mechanisms of load transfer can be made. The linear and unchanging correlation between the applied load and the total load transfer results from the fact that changes in frictional forces (that is, an increasing part of the load transferred by friction) are

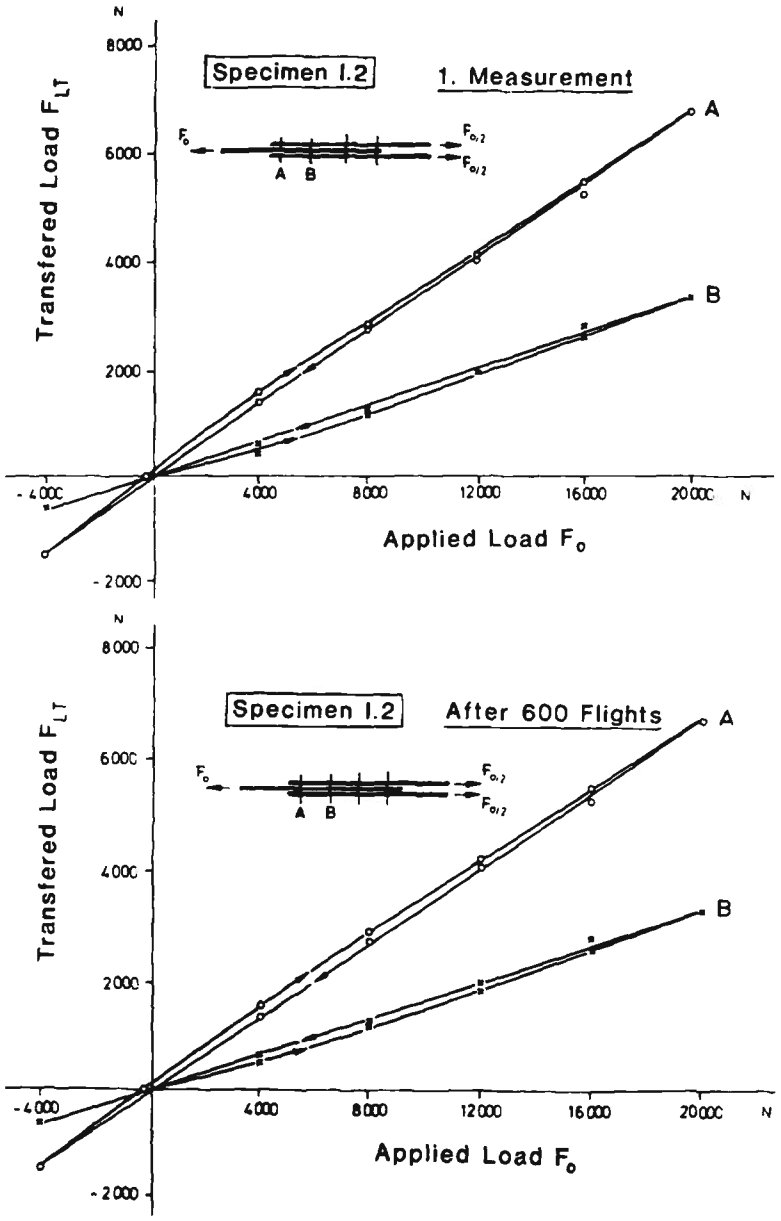

FIG. 14—*Influence of applied load and fatigue loading on the load transfer in a double-shear joint.*

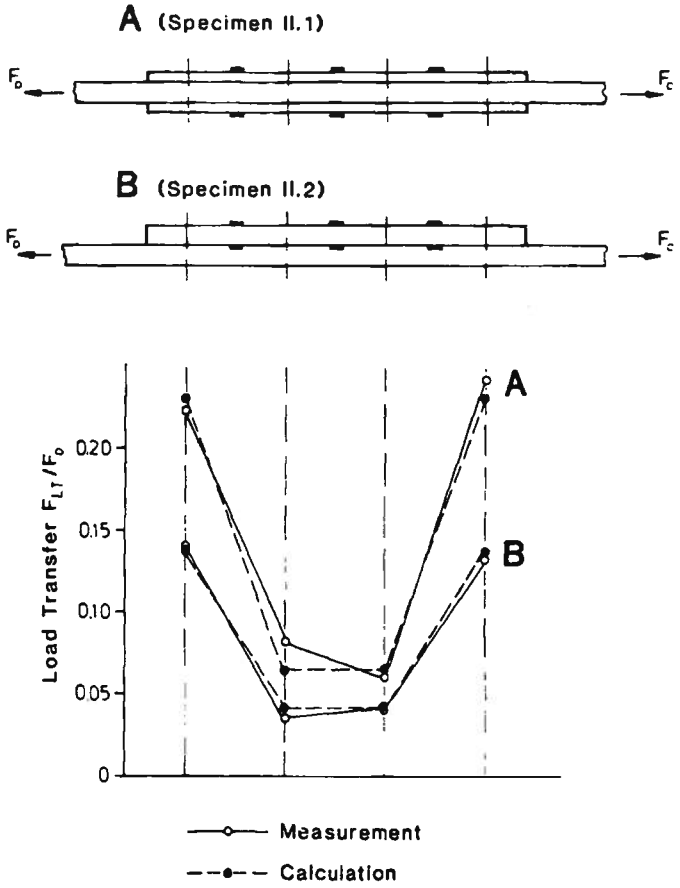

FIG. 15—*Distribution of fastener loads in four-row joints.*

accompanied by a decrease in the bearing load. This is illustrated schematically by the left sketch in Fig. 19.

Frictional forces, depending on clamping force and changing as a result of fatigue loading, also influence the notch root strains, as shown in the right sketch of Fig. 19. With increasing friction, the contribution from the bearing load to the local strain, and thus the total notch root strain, decreases. Redistributions of loads or changes in the load transfer mechanisms result in a relief of the critical volume of material at the edge of the fastener hole. Since the development and the effects of these changes cannot be predicted, the fatigue life cannot be accurately predicted using local stresses.

The following procedure is recommended for the fatigue life prediction of multiple-row joints. The distribution of fastener loads for the joint in question is to be calculated by taking into account the joint parameters and

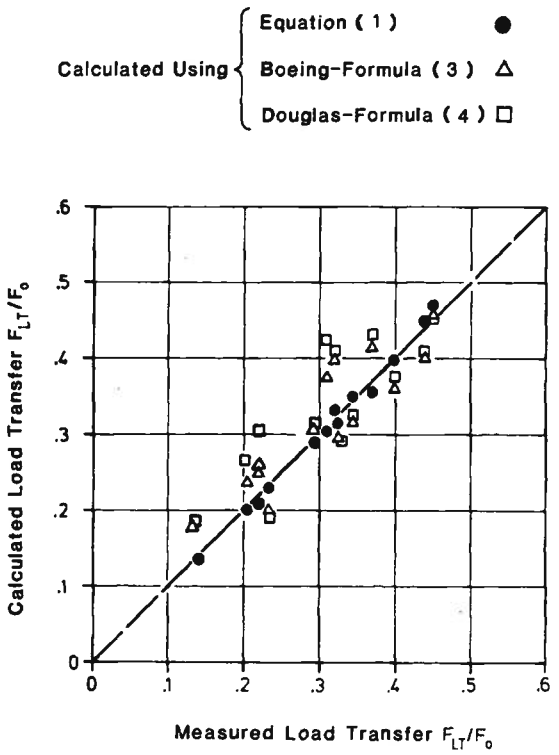

FIG. 16—*Comparison of measured and calculated load-transfer values for 13 different specimens.*

gross stresses. Then the respective stresses due to bypassing loads and the assumed bearing loads are determined. As shown before, a further calculation of local stresses or strains must be regarded as useless. More attention must be paid to the selection of the correct design data. These should be a set of life curves established for joint specimens of different load-transfer conditions and materials, using standardized flight-by-flight loading sequences. Influences on the fatigue behavior resulting from fastener installation parameters, secondary bending, the type of joint, and so on, are to be accounted for by experimentally determined correction factors. Finally, the relative miner's rule [*15*] can be used to account for the differences between the actual stress spectrum and the test spectrum of the design data.

Summary

The results of this investigation can be summarized as follows:

1. The influence of flight-by-flight loading on the deformation behavior and fastener flexibility of single- and double-shear joints is shown.

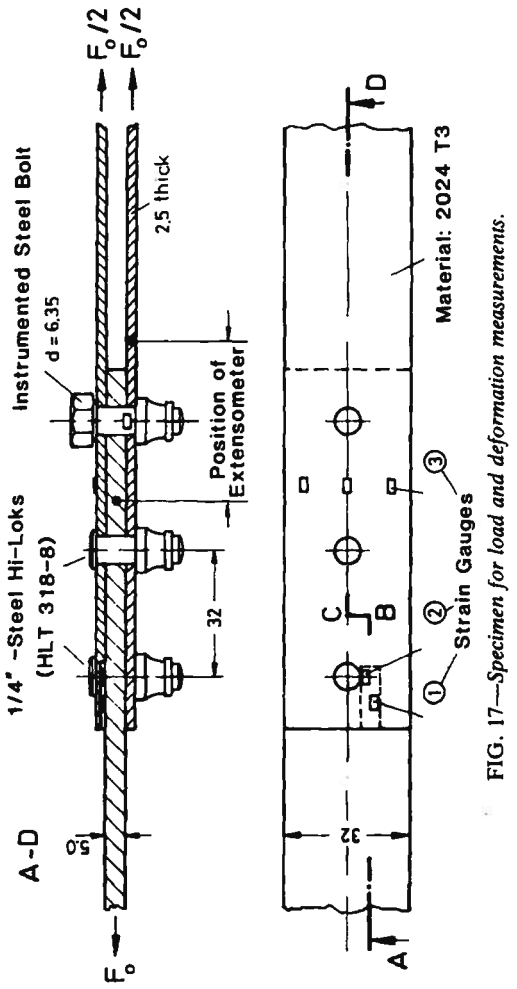

FIG. 17—*Specimen for load and deformation measurements.*

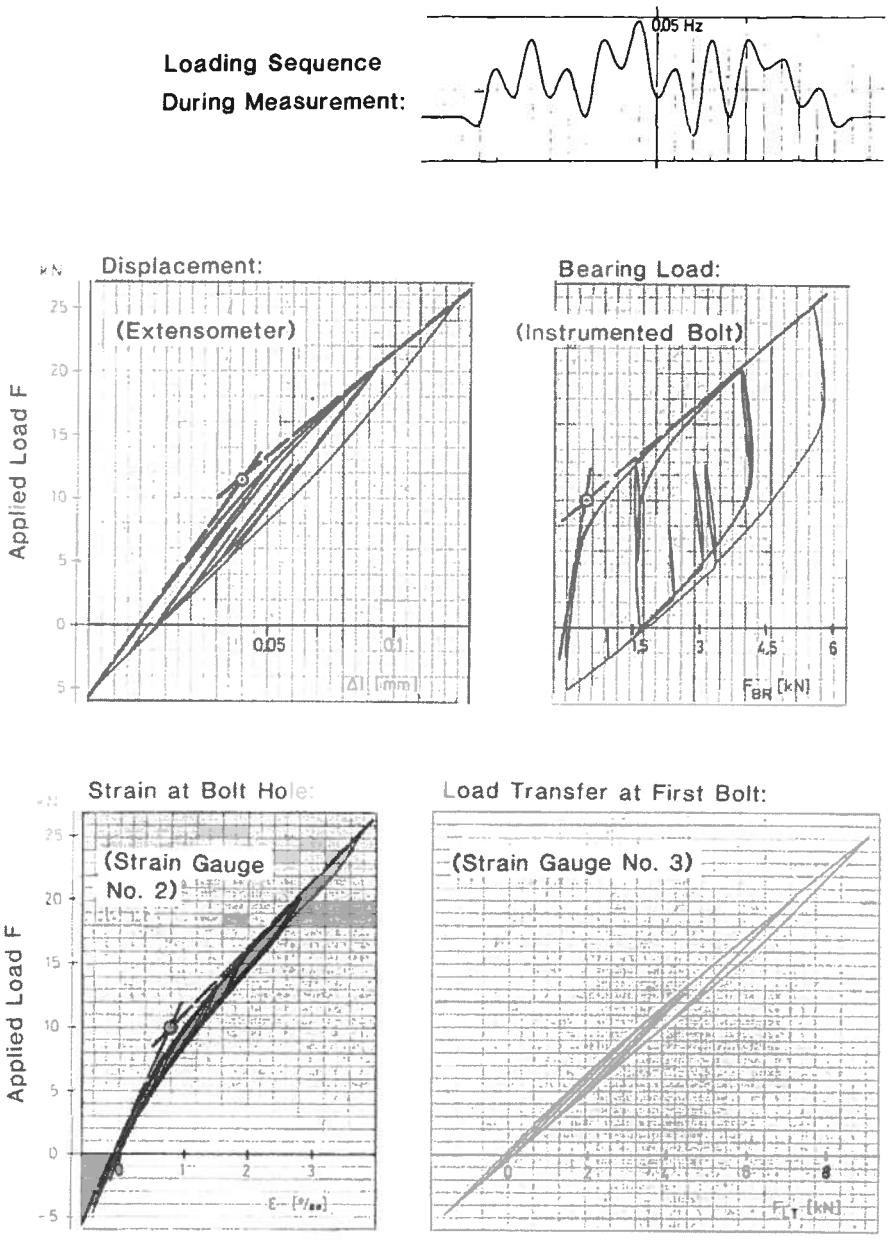

FIG. 18—*Measured loads and deformations in a double-shear joint.*

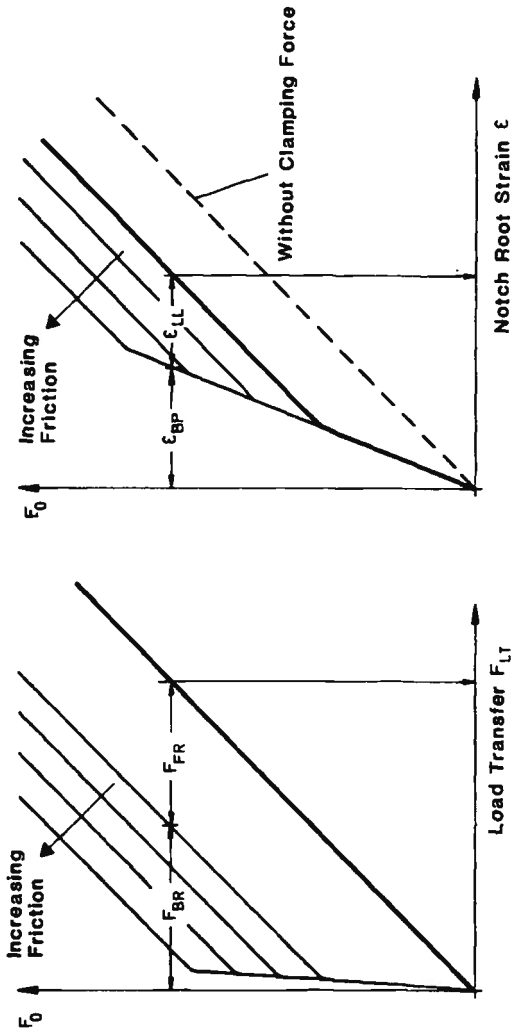

FIG. 19—*Mechanism of load transfer and its influence on notch root strain.*

2. A method for the evaluation of load-deformation curves is developed and a suitable definition of fastener flexibility to be used for loads transfer calculations of fatigue loaded joints is found.

3. For lap joints, the value of fastener flexibility can be regarded as a constant, since the total load transfer is independent of the stress level and the number of applied flights.

4. A new formula for fastener flexibility is derived. The use of this formula leads to improved load-transfer prediction and consequently also to improvements in fatigue life predictions for multiple-row joints.

5. The improved accuracy in load-transfer prediction will also have positive effects in the field of design and optimization of shear loaded joints.

6. From test results it can be concluded that the application of so-called local strain concepts for fatigue life predictions cannot be used successfully for joints.

7. The author suggests that to improve the accuracy in predicting the fatigue life of joints, fatigue data (S-N curves or life curves) incorporating stresses due to load transfer, bearing loads, and bypassing loads, together with a relative miner's rule, should be used.

References

[1] Bürnheim, H. "Beitrag zur Frage der Zeit- und Dauerhaltbarkeit der Nietverbindungen," dissertation, Technische Hochschule Darmstadt, Darmstadt, Germany, 1944.

[2] Jarfall, L., "Steel Bolts in Aluminum Plate: Fatigue Performance/Fastener Flexibility, FFA Report Hu-1369, Flygtekniska Försöksanstalten, Stockholm, Sweden, 1978.

[3] Franz, J. and Schütz, D., "Zur Lebensdauerabschätzung von Fügungen mit schubbeanspruchten Befestigungselementen unter Berücksichtigung der Lastübertragung," BMVg-FBWT 79-11, LBF, Darmstadt, Germany, 1979.

[4] Tate, M. B. and Rosenfeld, S. J., "Preliminary Investigation on Loads Carried by Individual Bolts in Bolted Joints," NACA TN-1051, National Advisory Committee for Aeronautics, Washington, DC, 1946.

[5] Vogt, F., "The Load Distribution in Bolted or Riveted Joints in Light-Alloy Structures," NACA Technical Memorandum No. 1135, National Advisory Committee for Aeronautics, Washington, DC, 1947.

[6] Franz, J., "Zur Spannungsanalyse von genieteten und geklebten Fügungen sowie von Sandwichplattenstreifen unter äußeren Lasten und Temperaturbeanspruchungen," LBF-Forschungsbericht FB-152, Darmstadt, Germany, 1980.

[7] Unpublished reports of the Boeing Co., Renton, WA.

[8] Barrois, W., "Stresses and Displacements Due to Load Transfer by Fasteners in Structural Assemblies," *Engineering Fracture Mechanics*, Vol. 10, Pergamon Press, 1978, pp. 115–176.

[9] Unpublished report of the Grumman Aerospace Corp.

[10] Swift, T., "Development of the Fail-Safe Design Features of the DC-10 in *Damage Tolerance in Aircraft Structures ASTM STP 486*, American Society for Testing and Materials, Philadelphia, 1971, pp. 164–214.

[11] Jarfall, L., "Review of Some Swedish Work on Fatigue of Aircraft Structures During the Period of May 1975 to April 1977," FFA Technical Note HE-1918, presented at the International Committee on Aeronautical Fatigue, Conference, Darmstadt, Germany, 1977.

[12] Jarfall, L., "Shear Loaded Fastener Installations," 12th International Committee on Aeronautical Fatigue, Symposium, Toulouse, France, 1983.

[13] Lowak, H., Schütz, D., Hück, M., and Schütz, W., "Standardisiertes Einzelflugprogramm für Kampfflugzeuge—FALSTAFF," IABG Report No. TF 568/LBF Report No. 3045, LBG, Darmstadt, Germany, 1976.

[14] Huth, H., "Zum Einfluß der Nietnachgiebigkeit mehrreihiger Nietverbindungen auf die Lastübertragungs- und Lebensdauervorhersage," LBF Report No. FB-172, dissertation, Technische Universität München, Munich, Germany, 1984.

[15] Schütz, W., "The Fatigue Life Under Three Different Load Spectra—Test and Calculations," AGARD CP-118, Symposium on Random Load Fatigue, Advisory Group for Aerospace Research and Development, Lyngby, Denmark, 1972.